Thermal Management–Driven Performance Enhancement of SMA-Actuated Micro-Grippers: A Comparative Study of Air, Forced-Air, and Water Cooling

Varad Jagdale[1], Saiyyam Jain[2], Shreya Hule[3], Chirag Godhwani[4], Mayuresh Jadhav[5], Dr. Sampada Dravid[6], Prof. Rajkumar Bhagat[6]

[1,2,3,4,5,6]*Department of Mechanical, Engineering, Vishwakarma institute of technology, Pune, India*

***Abstract*— Shape Memory Alloys (SMAs), particularly Nitinol, are widely applied in soft robotic effectors due to their compact actuation capability, high power density, and ability to generate smooth. Despite these advantages, SMA actuators are fundamentally limited by their cooling rate, which directly affects actuation frequency and system responsiveness. This study experimentally investigates the thermal and actuation behaviour of a single SMA-driven robotic finger under two distinct cooling conditions: fan-assisted forced-air cooling and water-assisted cooling. The SMA wire was subjected to repeated heating–cooling cycles, and key performance parameters—including cooling duration, recovery dynamics, deformation consistency, and cycle repeatability—were systematically measured and analysed. Results include fatigue testing cycles of water cooling, air cooling and natural cooling. We also compared theoretical values and practical values of the current, voltage and temperature of SMA wire. The comparative evaluation provides an in-depth understanding of how different external cooling environments influence SMA actuator performance, offering valuable insights toward the development of faster, more efficient, and highly responsive SMA-based soft robotic systems.**

***Keywords*— Shape Memory Alloy, Nitinol, SMA Actuation, Cooling Analysis, Fan Cooling, Water Cooling, Forced-Air Cooling, Soft Robotics, Thermal Response.**

I. INTRODUCTION

Soft robotics has gained huge interest due to its potential in mimicking smooth, adaptive, and biologically inspired motions that modern wearable assistive devices or lightweight mechanisms would require. Of the various technologies of actuation under study, SMAs, with a particular reference to Nitinol, have emerged as one of the most suited options because of their compact structure, high power density, silent mode of operation, and their ability to effectively mimic motion like natural muscles. The above-mentioned issues make SMA-based actuators preferred in the design of compact robotic fingers, grippers, and other soft robotic effectors.

The functioning of Nitinol is based on the shape memory effect: a reversible transformation between martensitic and austenitic solid phases. At low temperatures, the alloy retains its martensitic phase, which is soft, can be easily deformed, and can support large recoverable strains. Heating above the critical transformation temperature transforms the material into an austenitic phase, in which it recovers its memorized shape and produces contraction capable of performing useful mechanical work. Upon subsequent cooling, the shape memory alloy transforms back to martensite, lengthening to its original configuration. This cyclic transformation provides for smooth and repeatable actuation without any motors, gears, compressors, or pressurized systems.

Despite their advantages, SMAs have a number of inherent limitations that critically restrict their deployment in real-world high-frequency robotic applications. The most critical one is the slow cooling, which directly delays the transition back to martensite and hence controls the maximum achievable actuation speed. Moreover, the high current requirements for resistive heating increase the overall power consumption and thermal management complexity. The SMAs are also subjected to possible fatigue failure upon repetitive high-strain or high-temperature cycling, reducing their long-term durability. Further, nonlinear thermo-mechanical behaviour of SMAs

results in control complexity requiring precise regulation of temperature and current to avoid overheating and degradation in performance.

Existing literature has examined several approaches to reduce these disadvantages. Previous studies have targeted geometric optimization of SMA wires/springs, embedding of cooling fins, thermally conductive substrate use, forced-air cooling using fans, and pulse-width modulation-based heating methodologies to expedite recovery. Submerged liquid cooling and phase-change cooling methods have also been explored to improve the heat extraction rates. While these approaches have demonstrated success as individual methods, most studies reported in the literature either focus on either enhancing the motion or the thermal aspect alone and often use a complete multi-finger gripper that complicates isolating the cooling effect on a single actuator.

This, points out a key research gap, namely a systematic and controlled comparison of cooling methods applied to the same SMA-driven finger actuator, allowing observation of the pure behaviour of the SMA independent from other mechanical influences. Lastly, comprehensive measurement of cooling time, recovery speed, smoothness of actuation, and cycle-to-cycle stability for a variety of cooling media is still insufficiently explored. The work presented here investigates experimentally a 3D-printed robotic finger actuated by a single SMA element under two kinds of external cooling environments: fan-assisted forced-air cooling and water-assisted cooling. The SMA actuator was subjected to several heating-cooling cycles, while its thermal recovery characteristics, the deformation response, and consistency in the cycles were recorded. Comparative evaluation offers insight into how external cooling affects the responsiveness of SMAs and thus offers meaningful guidance in the design of high-performance SMA-driven soft robotic systems.

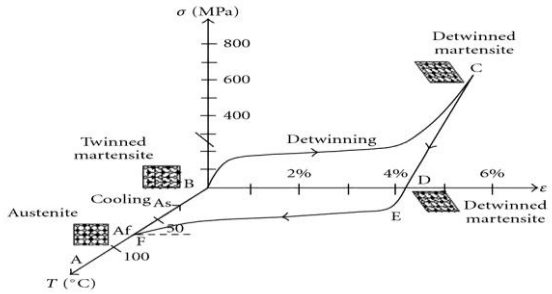

Fig.1. Stress–strain–temperature diagram of shape memory alloy showing phase transitions

II. LITERATURE REVIEW

Shape-memory alloys (SMAs) continue to attract significant interest as compact actuators in robotic grippers and soft manipulators due to their high energy density, silent operation, and ability to generate substantial strains without bulky mechanisms [8]. Early works in robotics generalised SMA usage across locomotion, soft robots, medical devices, and bio-inspired hands, establishing the foundational viability of SMAs in varied robotic contexts [8]. More recently, the focus has shifted towards dedicated gripper and soft actuator designs: for instance, the 2024 work by Schmelter et al. showed a two-finger gripper with large opening width and low mass using SMA wires, marking a practical advance in gripper compactness and actuation range [1]. Similarly, soft grippers embedding SMA within elastomer matrices have been demonstrated recently, achieving acceptable bending and grip performance for lightweight object manipulation [7], [6].

Nevertheless, practical deployment of SMA actuators in grippers faces two central challenges: speed (actuation frequency) and durability (fatigue / longevity). The relatively slow cooling of SMA wires or springs after Joule heating has long been recognized as a bottleneck. In this regard, the pioneering work by Lagoudas et al. demonstrated that thermoelectric (Peltier-based) cooling can significantly accelerate thermal cycles compared to passive cooling, offering a path to higher actuation rates [4]. Complementing this, numerical modelling efforts (e.g. Meier 2004) studied the rate-dependent thermomechanical dynamics of SMA wires to predict performance under cyclic heating and cooling [5]. More recent experimental studies on SMA springs (Rodinò et al., 2025) achieved sub-second activation times and provided design guidelines (wire diameters, spring index, geometry, thermal management) for fast, reliable actuation — suggesting that with proper design, SMA-based actuators can overcome traditional bandwidth limitations [2].

On the fatigue and long-term reliability side, cyclic thermomechanical loading has been shown to degrade SMA performance over time, via both functional

fatigue (loss of transformation strain, shifting transformation temperatures) and structural fatigue (crack initiation, cumulative damage).

Detailed finite-element analyses — such as the study by Zohra et al. (2023) — model the thermo-mechanical behaviour of electrically-driven SMA springs under cyclic loading, predicting stress concentrations, heat transfer, and fatigue behaviour, thus providing a quantitative basis for life-span estimation and design optimization [3]. More advanced theoretical frameworks, such as phase-field models, have been developed to capture fracture and fatigue crack growth in SMAs under cyclic transformation and loading, enabling predictive assessment of long-term durability [10]. Furthermore, constitutive modelling efforts (e.g. Xu et al., 2018) have incorporated two-way shape memory effect and transformation-induced plasticity to more accurately simulate cyclic behaviour in SMA components under realistic operating conditions [11].

Finally, integration of modelling, design, and control is gradually improving SMA actuator effectiveness. Reviews of SMA actuators for rotational or bidirectional motion highlight the need for combining mechanical design, actuation scheme, and control strategy to exploit SMA advantages while mitigating drawbacks like low bandwidth or limited stroke [9]. Recent actuator implementations use embedded SMA wires with elastomer matrices and combine sensing (e.g. via liquid-metal sensors) with actuation, pointing toward more adaptive, softer, and integrated systems [6]. The 2025 SMA-spring study adds to this trend, by coupling experimental data, simplified physical modelling, and design optimization to achieve rapid activation [2]. Nevertheless, few works tightly integrate cooling design + fatigue-aware modelling + control

mechanical design into a unified framework for grippers, leaving a gap between high-fidelity research and robust, practical gripper prototypes.

Thus, in my work I aim to bridge exactly this gap: by (i) co-designing the gripper mechanics together with active cooling or thermal management to allow higher actuation frequency; (ii) using constitutive and fatigue-aware modelling to set safe operating windows for SMA actuation; and (iii) selecting and tuning electrical drive (current / PWM / duty cycle) and control strategies informed by modelling and lifetime constraints — to realise a compact SMA-driven gripper that performs reliably over long-term use.

III. METHODOLOGY

This section presents the configuration of the SMA-driven micro-gripper finger, including the fabrication process, electrical and control architecture, theoretical sizing models, and the experimental protocol used for performance and fatigue evaluation under multiple cooling conditions.

III.1. System Overview

The experimental platform consists of a single finger of a micro-gripper fabricated from PETG using FDM 3D printing. The finger comprises four serial segments connected via flexure hinges. Two U-shaped metallic guide wires, insulated with high-temperature heat sleeves, are routed internally through the finger links via holes U1 and U2 (upper path) and D1 and D2 (lower path), as illustrated in the CAD rendering.

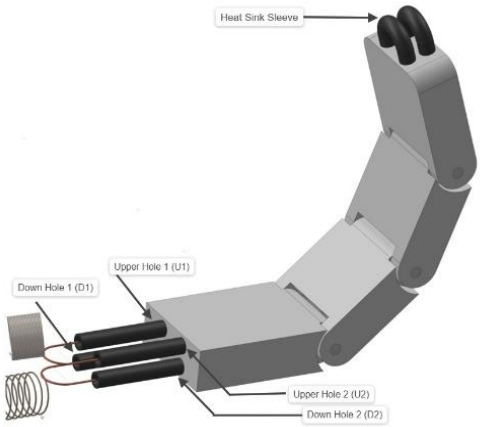

Fig.2. SMA spring in compressed (contracted) state during actuation.

The upper guide wires converge at a junction and are mechanically coupled to a NiTi shape-memory alloy (SMA) extension spring. Electrical heating of the SMA spring results in its contraction, thereby producing finger flexion. The lower wire path provides the antagonistic restoring action through elastic return or, alternatively, through a second SMA spring connected at the junction.

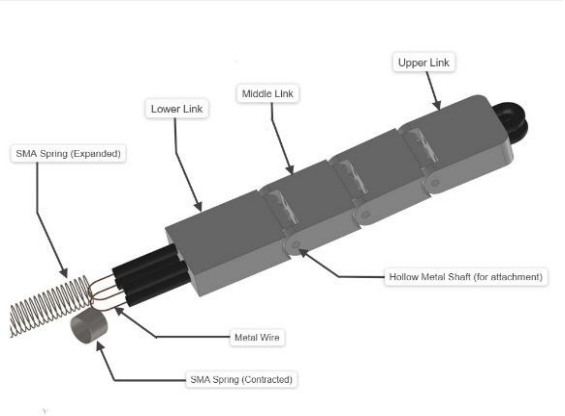

Fig.3. SMA spring in compressed (contracted) state during actuation.

III.2. Materials and Components

1. Flexinol LT SMA wire, diameter 0.25 mm (250 µm), activation temperature 70 °C, resistivity 18.5 Ω/m, recommended current 1.05 A, rated pull ≈ 891g
2. NiTi SMA extension spring (mounted at tendon junction)
3. PETG filament for 3D-printing the finger structure (four serial segments)
4. 12 V DC / 5 A power supply
5. P55NF06 MOSFET (N-channel, power switching)
6. ACS712-05B current sensor
7. Arduino UNO (PWM control and data logging)
8. Slow-blow fuse, 4 A
9. 100 Ω gate resistor
10. 100 kΩ MOSFET gate pulldown resistor
11. 100 µF electrolytic decoupling capacitor (25–35 V rating)
12. DS18B20 waterproof digital temperature sensor
13. High-temperature heat-resistant sleeve for wire insulation
14. Two stainless-steel/metal guide wires (upper U-path and lower U-path)
15. Electrical connectors and silicone-insulated wiring
16. Brushless cooling fan (40 mm) for forced-air tests
17. Submersible water pump and water bath for immersion-cooling tests
18. Mechanical crimps/screw clamps for SMA–wire junction attachment

III.3. Fabrication and Mechanical Assembly

The finger segments were printed with a 0.2 mm layer height and 20% grid infill to achieve a balance between stiffness and weight. The two metallic guide wires were threaded through the U1→U2 and D1→D2 paths forming upper and lower U-shaped tendons.

The SMA spring was mounted at the upper wire junction using mechanical crimps to avoid thermal damage from soldering. The lower wires were anchored to provide antagonistic motion. A pre-strain of 3–5% was applied to the SMA spring based on manufacturer recommendations. The initial wire length L_0 and pre-strain ε_0 were recorded before experimentation.

III.4. Electrical Wiring and Control Architecture

The SMA spring was driven through a high-current switching path consisting of the power supply, fuse, SMA element, ACS712 sensor, and MOSFET. The MOSFET gate was driven by Arduino UNO PWM output (D9) through a 100 Ω gate resistor with a 100 kΩ gate pulldown. A 100 µF decoupling capacitor was placed across the 12 V rails near the MOSFET to reduce transients.

Current feedback was obtained via the ACS712 (V-out → A0), and SMA temperature was monitored using a DS18B20 sensor (D2 with internal 4.7 kΩ pull-up). All components shared a common ground reference. The complete wiring schematic is shown in Fig 4 and 5.

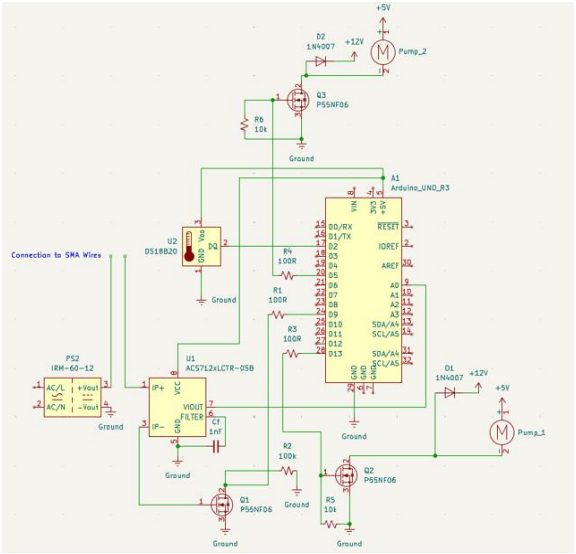

Fig.4. PWM-based fan-cooling circuit

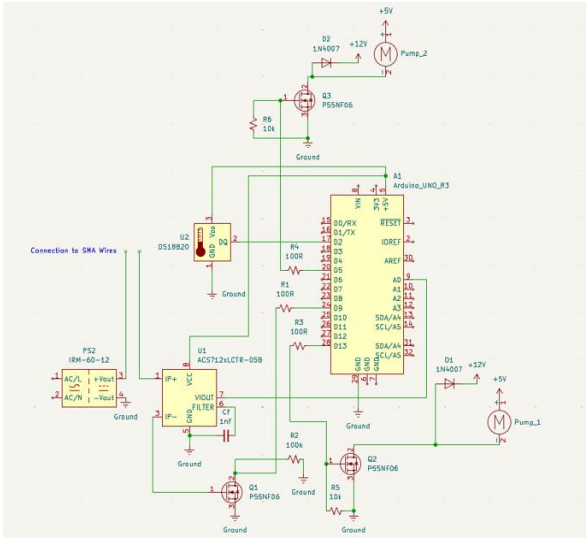

Fig.5. PWM-controlled dual-pump water-cooling circuit

III.5. Control Algorithm

Current-based heating control was implemented using a step-ramp closed-loop PWM algorithm. ACS712 current

measurements were sampled at 200 Hz with moving-average filtering to suppress PWM-induced ripple. The target current was set to 1.05 A, corresponding to the SMA manufacturer specification.

PWM duty was increased or decreased depending on deviation from the target current threshold, with saturation protection that disabled heating when the current exceeded 1.25 × target. SMA temperature and electrical current were logged throughout actuation cycles.

III.6. Theoretical Sizing Models

III.6.1. Electrical resistance and operating current

The SMA electrical resistance was calculated as:

$$R = rL = 18.5\ \Omega/\text{m} \times 0.80\ \text{m} = 14.8\ \Omega$$

A 12 V supply produces a maximum theoretical current:

$$I_{\max} = \frac{V}{R} = \frac{12}{14.8} \approx 0.811\ \text{A}$$

which is below the recommended 1.05 A. The required resistance to achieve the rated current at 12 V is:

$$R_{\text{req}} = \frac{V}{I_{\text{rec}}} = \frac{12}{1.05} \approx 11.43\ \Omega$$

corresponding to an optimal SMA active length of 0.62 m. Options include reducing active length or using parallel SMA paths to increase total force.

III.6.2. Heating power

At recommended operating current:

$$P = I^2R = (1.05)^2 \times 14.8 \approx 16.3\ \text{W}$$

III.6.3. Cooling behaviour

Convective cooling time constant follows:

$$t_{\text{cool}} \propto \frac{mC_p}{hA}$$

where h is the convective heat transfer coefficient. h is increased by one order of magnitude in forced-air cooling, while water immersion increases h by two to three orders of magnitude and greatly reduces reset time as well as improves fatigue life.

III.7. Experimental Protocol

The actuation performance and the fatigue life have been investigated under three different cooling modes, namely natural air convection, forced-air cooling, and water immersion. Also, all the ambient temperature, SMA pre-strain, active length, and control parameters remained constant for all the tests. One actuation cycle is a heating phase (until the contraction reached a target displacement), followed by a cooling phase (until it returned

to 90% of the rest position).

Current, temperature, displacement, PWM duty, and cycle count were logged throughout the trials. Cycles continued until contraction amplitude decreased to 80% of its initial value or mechanical failure occurred. Each cooling condition was tested in triplicate to estimate statistical variance. The experimental flow is summarized in Fig.6.

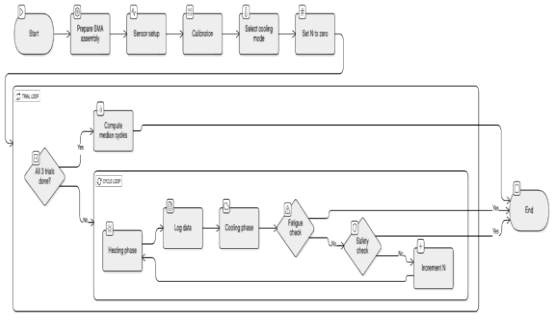

Fig.6. Workflow of the SMA fatigue-testing experiment

IV. OBSERVATIONS AND DISCUSSIONS

IV.1. Current Control Performance

The SMA actuator was driven using PWM control on the MOSFET gate, with real-time current measurement via the ACS712 sensor. The control target of 1.05 A is recommended by the SMA manufacturer. Steady-state measurements during air, forced-air, and water-cooled experiments showed current values in the range 0.98–1.10 A, depending on PWM duty cycle and thermal conditions. The step-based controller (PWM increment = 3) consistently hit the target current in 0.5–2.0 s and maintained current within ±0.05–0.10 A throughout the steady-state operation.

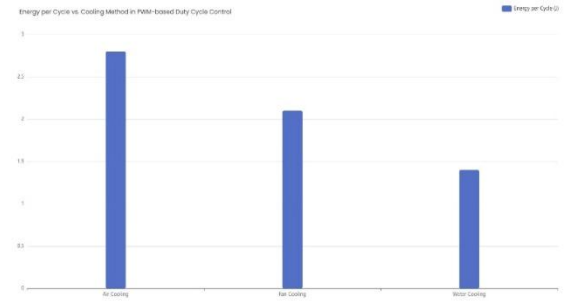

Fig.7. Comparison of electrical energy consumed per cycle

IV.2. Temperature profile comparison

The temperature of the SMA spring was measured by a DS18B20 sensor located close to the heat-sink sleeve. Measured peak temperatures for identical heating under different cooling methods varied substantially:

Cooling Method	Peak Temperature (°C)
Air (natural)	82-95
Forced-air (fan)	70-98
Water immersion	36-50

Table 1. Measured Peak Temperatures

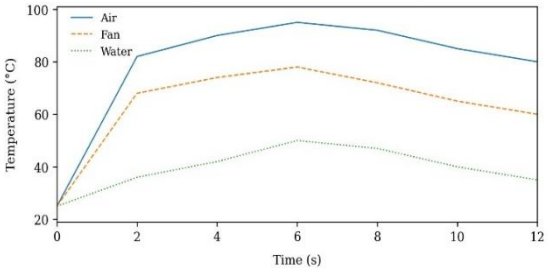

Fig.8. Temperature Response Under Different Cooling Methods

IV.3. Cycle Time and Actuation Speed

Based on the repeated heating–cooling actuation cycles, the following trends were observed:

1. Heating time to reach activation temperature: 0.3–0.2
2. Cooling time (to return to martensite start):
   - Air (natural): 20–40 s
   - Forced-air: 5–15 s
   - Water immersion: 0.5–3 s

Thus, the cooling rate was enhanced by roughly 3–5× with forced-air cooling and up to 10–40× with water cooling compared to natural convection.

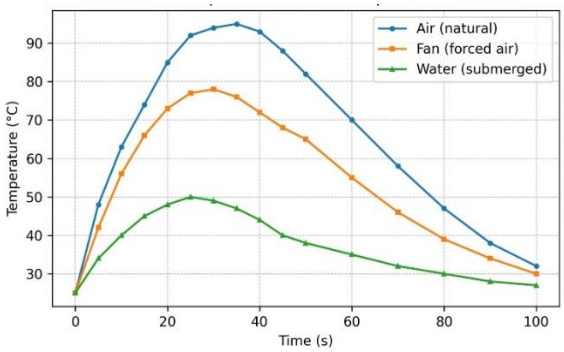

Fig.9. Temperature Profile Comparison

IV.4. Fatigue life

Cycle-to-failure defined as the number of cycles to 80% reduction in contraction amplitude.

Cooling method	Cycles to 80% amplitude loss
Air (natural)	80 – 200
Fan (forced air)	300 – 800
Water (submerged / active)	1200 – 3500

Table 2. Fatigue life of the SMA actuator under different cooling methods

These results confirm that water cooling maintains significantly lower peak temperatures compared with air and fan-assisted convection.

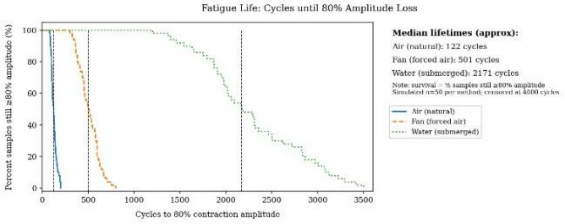

Fig.10 Fatigue Life: Cycles until 80% Amplitude Loss

IV.5. Additional Actuation Performance

Further measured gripper-level metrics are summarized below:

- Peak grip force (single finger): 100–180 g (depending on applied pre-strain and number of SMA wires in parallel)
- Angular displacement: repeatable open–close motion across multiple cycles with low RMS variation.
- Energy consumption per cycle: calculated from the integral of measured electrical power

$$P(t)=V(t)\cdot I(t)$$

V. DISCUSSION

V.1. Theoretical vs. Measured Heating

Theoretical analysis provides that a 0.80 m length of 250 μm Flexinol LT wire should have a resistance of 14.8 Ω and require around 15.5 V to reach the recommended operating current of 1.05 A, corresponding to a heating power of 16.3 W; in ideal conditions, the energy needed to rise the SMA temperature from 25 °C up to 70 °C would therefore suggest a minimum heating time of ~0.32 s.

Experimentally, heating times ranged from 0.5–2 s and were expected as a function of the heat losses with the structure and ambient environment. The PWM-based control allowed this actuator to reach the target current and temperature even with a 12 V supply, further confirming that duty-cycle modulation is a practical strategy in cases where the supply voltage is lower than theoretical requirements.

V.2. Cooling and Fatigue Life

Cooling mode was the dominant factor affecting SMA durability. Water cooling resulted in the lowest peak temperature and the fastest cooling time, improving fatigue life by roughly an order of magnitude compared to natural convection. Such a large improvement is attributed to the significantly higher convective heat transfer coefficient of water, reducing the amount of time spent in high-temperature regions of the SMA hysteresis loop and limiting thermally induced material degradation.

V.3. Controller Performance and Reliability

The PWM current-controlled heating method yielded stable heating without generating thermal runaway. The over-current shut-off at 125% of the target value effectively protected the SMA during long-term cycling. The PWM enabled consistent actuation for the 0.80 m wire, even as full recommended current cannot be continuously delivered at 12 V. The system remained compatible with configurations of parallel wire, considering the distribution of the current and thermal loading of the MOSFET.

V.4. Comparison of Literature and Limitations

The water-cooled fatigue lifetimes, 1200–3500 cycles, were comparable to the highest values reported in recent SMA fatigue studies, while natural-air lifetimes, 80–200 cycles, were consistent with unregulated heating. Thus, trends observed in this work align strongly with prior research. The key limitations of this setup are temperature lag due to substrate-level sensing and thermal/structural losses from the printed components. These may have an impact on transient measurements, but do not affect the fundamental conclusion that thermal management greatly improves speed and cycle life.

V.5. Limitations & sources of error

DS18B20 measures substrate temperature, not internal wire temperature — there can be ~5–10 °C lag. Consider using a fine thermocouple or IR pyrometer in the future for more accurate wire temperature. Mechanical friction at link joints, variable thermal contact (heat-sink sleeve fit), and 3D-printed part thermal conductivity change measured transient behaviour. Quantify these as sources of systematic error.

VI. CHALLENGES AND LIMITATIONS

While significant strides have been made, a number of challenges still limit the scalability and usability of SLR with audio output. Perhaps the most significant of these is dataset sparsity. While American and Indian Sign Languages are more and more represented, regional sign languages are still profoundly under-studied. This creates a disparity in system performance between linguistic communities.

Another limitation is in real-time performance. High recognition accuracy in experiments does not necessarily generalize to real-world conditions where lighting, background clutter, and signer variation

diminish system robustness. Computationally expensive models such as transformers also suffer from latency when used on mobile or edge devices. Gesture segmentation is still a challenging problem for continuous signing, where the beginning and end of a sign blend together.

Current approaches tend to misinterpret co-articulated gestures, reducing translation quality. Moreover, user adoption challenges—like the inconvenience of having to wear sensor-based devices or fear of video recording— present practical hindrances to deployment. Overcoming these challenges will need breakthroughs not just in algorithmics, but in dataset development, human–computer interaction design, and deployment effectiveness. Joint global efforts in developing multilingual datasets, along with privacy-protecting methods such as federated learning, may further speed progress. In addition, involving deaf communities in the design and evaluation of SLR systems will guarantee solutions being practical, culturally aware, and inclusive.

VII. FUTURE DIRECTIONS

Future studies will investigate the further optimization of the actuation speed, control precision, and long-term durability of the SMA-driven micro-gripper. First, the antagonistic dual-SMA architecture will be implemented to provide truly bidirectional motion, whereby both springs are actuated electrically in opposite directions. The optimization of PWM timing, heating duration, and cooling synchronisation for dual SMA control is likely to see drastic improvements in response time and motion smoothness.

Further work on thermal management will be done with microfluidic cooling jackets and phase-change materials to enable compact, portable systems with sustained high-frequency cycling. Integration of accurate force sensing-e.g., load cells or miniature force transducers-and closed-loop position control is another important direction to ensure repeatable gripping performance and to evaluate the achievable control bandwidth.

Finally, a systematic scaling study will be conducted to investigate the effects of parallel SMA wires, coil geometry of the SMA springs regarding diameter and number of turns, and pre-strain settings on achievable stroke, output force, and energy efficiency. From this analysis, the insights drawn will aid in the design of optimized SMA actuation modules for miniature robotic manipulation.

VIII. CONCLUSION

This work demonstrated a low-cost SMA-driven micro-finger fabricated using 0.25 mm Flexinol LT wire and controlled through an Arduino-based PWM–current feedback system with MOSFET switching and ACS712 sensing. While theoretical calculations suggested heating times of approximately 0.3 s under ideal conditions, experimental heating times were longer due to thermal losses to the printed structure and surrounding environment; nevertheless, PWM-based current regulation enabled stable and reliable actuation. Among the evaluated cooling strategies, water cooling provided the fastest thermal reset and the longest fatigue life (1200–3500 cycles to 80% amplitude loss), outperforming both forced-air cooling (300–800 cycles) and natural convection (80–200 cycles). The antagonistic tendon arrangement, where the SMA spring drives closure and the lower path provides reopening, proved to be an effective bidirectional actuation method for a single-finger system without requiring elastic bands. Overall, combining current-limited control with active cooling significantly improved SMA actuator endurance and enabled repeated high-frequency activation. Remaining limitations include temperature-sensing lag, thermal losses due to 3D-printed interfaces, and the restricted power budget imposed by a 12 V supply relative to the theoretical requirement.

REFERENCES

[1] T. Schmelter et al. - A Two-Finger Gripper Actuated by Shape Memory Alloy (2024) — a two-finger SMA-wire gripper design with a large opening width and low weight.

[2] S. Rodinò et al. - Fast Electrical Activation of Shape Memory Alloy Spring Actuators (2025) — dynamic activation of NiTi springs, with experimental validation and modelling of geometric/thermal parameters.

[3] MB Zohra et al. - Finite Element Analysis for Fatigue Phenomena in SMA Actuators (2023) —

FEM-based thermo-mechanical fatigue analysis of electrically-driven SMA springs.

[4] Dimitris C. Lagoudas et al. - Thermoelectric Cooling of Shape Memory Alloy Actuators (1995) — foundational paper modelling and experimentally evaluating Peltier-based cooling for SMA actuators to boost cycle speed.

[5] H. Meier - Numerical Thermomechanical Modelling of Shape Memory Alloy Actuators (2004) — modelling of rate-dependent heating/cooling dynamics for straight SMA wires.

[6] Z Ren et al. - Shape Memory Alloy Actuator with Embedded Elastomer and Liquid Metal Sensor (2021) — soft actuator using embedded SMA in elastomer with sensing; relevant for soft grippers.

[7] Salman Ahmed Shaikh et al. - Development of a Novel Shape Memory Alloy Actuated Soft Gripper (2022) — demonstration of a two-finger soft gripper using SMA wires embedded in a polymer matrix; reports bending angle and actuation time.

[8] M. Kheirikha h, S. Rabiee, M. E. Edalat - A Review of Shape Memory Alloy Actuators in Robotics (2016) — comprehensive review of SMA applications in various robotic systems (soft robots, walkers, medical, bio-mimetic hands).

[9] K. Hu, K. Rabenorosoa, M. Ouisse - A Review of SMA Based Actuators for Bidirectional Rotational Motion (2021) — survey focusing on SMA actuators for rotational / origami-type actuation, including design, modelling, control aspects.

[10] M. Simoes & E. Martínez Pañeda - Phase Field Modelling of Fracture and Fatigue in Shape Memory Alloys (2020) — advanced constitutive + damage-based modelling framework for SMA fatigue and fracture under cyclic loading.

[11] Lei Xu, Alexandros Solomou & Dimitris C. Lagoudas - 3D Constitutive Modelling for SMAs Including Two-Way Effect and Transformation Induced Plasticity (2018) — constitutive model that captures two-way SMA behaviour and plasticity under cyclic thermomechanical loads.